

Modeling of nitrogen and phosphorus profiles in sediment of Osaka Bay, Japan with parameter optimization using the polynomial chaos expansion

Masayasu Irie ^a, Fumiaki Hirose^a, Teruhisa Okada ^b, Jann Paul Mattern ^c and Katja Fennel ^d

^aDepartment of Civil Engineering, Osaka University, Suita, Japan; ^bEnvironmental Science Research Laboratory, Central Research Institute of Electric Power Industry, Abiko, Japan; ^cDepartment of Ocean Sciences, University of California, Santa Cruz, CA, USA; ^dDepartment of Oceanography, Dalhousie University, Halifax, Canada

ABSTRACT

Coastal sediments adjacent to urban centers often receive high loads of organic matter (OM) due to large nutrient inputs from land that stimulate algae blooms. Early diagenetic models describing the remineralization of this OM in sediments have been developed for 50 years. Although these models can be applied to a range of marine sediments, specifying their model parameter values is difficult. In this study, one of the early diagenetic models was applied to simulate sediments in Osaka Bay, Japan and the polynomial chaos expansion (PCE) technique was used in order to choose optimal model parameters in the model. Following a sensitivity analysis, we estimated values for six parameters including the ratio of fast-decaying OM to total OM, the ratio of non-degradable OM to total OM, and the carbon–nitrogen ratio. Optimal parameter values were determined by minimizing the misfits between simulated and observed release rates of ammonium and phosphate from the sediments, and vertical profiles of inorganic nitrogen, and phosphorus in the porewater. Simulations with the optimized parameters successfully reduce a dimensionless root mean square error by 68% and agree better with the observed profiles and release rates than without parameter estimation.

ARTICLE HISTORY

Received 24 November 2017
Accepted 30 September 2018

KEYWORDS

Polynomial chaos expansion;
early diagenesis model;
nutrient release; sediment;
Osaka Bay

1. Introduction

Over the past several decades, estuaries and lakes in Japan have been subjected to heavy nutrient loads from highly urbanized areas. Although various laws and regulations to control nutrient discharge have been enacted and enforced since the 1960s, policies such as the construction of sewage treatment plants could not meet the increase in nutrient loads. Today, sanitation systems cover 77.8% of the population in Japan with sewerage lines and this coverage reaches 89.9% when including septic tanks and rural community sewerages (Ministry of Environment, Government of Japan, 2016). Tada et al. (2014) reported that the concentrations of nutrients have recently decreased in the eastern part of the Seto Inland Sea, which includes Osaka Bay a target area in this study in the east end. Marine sediments, however, contain large amounts of organic matter due to excessive nitrogen and phosphorus loads and the resulting primary production and sedimentation of organic matter. Osaka Bay has been affected by large nutrient loads from rivers such as the Yodo River, the Kanzaki River, and the Yamato River, and, as a result, high concentrations of organic matter are contained in its seabed. Joh (1986) reported that, based on ignition loss measurements, organic matter made up 5–13% of the bottom mud

across the bay in the 1960s. The organic matter fraction continues to be high with recent values of 5.0–9.4% in 2016 (Ministry of Land, Infrastructure, Transport and Tourism, Government of Japan, 2017). Yokoyama and Sano (2015) reported, after field surveys, that the total organic carbon and total nitrogen in the sediment were greater than 18 and 2.4 mg g⁻¹, respectively, at the head of the bay. Further, the study indicated that the area where these values are high has not changed since 1975. In addition to nutrient loads from land, the complexity of coast lines and the construction of wharfs and breakwaters for use of the coastal area as ports contribute to high organic matter contamination of the sediment. Construction has produced areas where the flow velocity is slow and has reduced shallow areas where the depth is less than 10 m. In such areas, it is easy for algal blooms to occur causing detritus to sink down onto the seabed. Irie, Nakatsuji, and Teranaka (2007) reported that sediment oxygen consumption rate (Sediment Oxygen Demand (SOD)) reaches 10 g m⁻² d⁻¹ just outside a port located in Osaka Bay. These field surveys reveal a large amount of organic matter is accumulated in the head of the bay.

Nutrient release from the seabed plays a major role in primary production and material circulation in coastal seas. The release rate of ammonia–nitrogen

(NH₄-N) from the seabed is 13.2–1164 mg m⁻² d⁻¹ in the eastern part of the bay where there is excessive primary production, and up to 6.9 mg m⁻² d⁻¹ in the western part of the bay, where the current is vertically uniform and the water is relatively clean due to water exchange through the straits and smaller impact of loadings from land than in the eastern part. Even though a number of field surveys and laboratory experiments were carried out and the release rates were examined, the quantification of water-bed interactions is complicated by the wide range of measured rates. The causes for such the large variety of the rates is not clear, but possibly it is a representation error because the number of core samples is very limited and the characteristics of the bottom mud differ by sampling location even over small distances (Blair and Aller, 2012; Canfield, 1994).

To help us clarify the physics and biogeochemistry of nitrogen and phosphorus and their exchange between sea water and the mud, numerical modeling plays an important role. Early diagenesis models have been developed in the early stages of modeling sedimentation and material circulation in the sediment. The early diagenesis model is able to reproduce the vertical profiles of materials in the porewater and sediment (Wijsman et al., 2002; Berg, Rysgaard, and Thamdrup, 2003; Fossing et al., 2004). The model sometimes lacks the reproducibility of the diffusion of materials from the mud to sea water. Irie et al. (2010) used an early diagenesis models to estimate SOD, which is the sum of the direct consumption at the sediment surface and the release of reducing substances such as hydrogen sulfide, at the head of Osaka Bay. Although the spatial trend of the simulated rates over the sampling sites is similar to the measured laboratory rates, the simulated magnitudes were much different. It can be noted that it is sometimes difficult for early diagenesis models to reproduce the vertical profiles of nutrients and the release rates of nutrients simultaneously. While the model's wide range of parameters and boundary conditions can accommodate a range of model settings, increasing the flexibility of this type of model, setting the model parameters and boundary conditions takes a lot of effort (see, e.g. Wilson, Fennel, and Mattern (2013); Laurent et al. (2016)). Especially when there are insufficient observations and laboratory measurements, constraining the parameter values becomes rather difficult. Moreover, as Boudreau (1997) remarked, various types of models with these processes have been developed to model marine sediments. While it is difficult to obtain useful and sufficient field and experimental data for a specific model at a given time and location, it is also difficult to select the best model for the data that was already collected. A suitable combination of field data and model are necessary to better learn the material cycles in sediment.

Polynomial chaos expansion (PCE), also known as Wiener chaos expansion firstly introduced by Wiener (1938), is a statistical emulator that can be used to set model boundary conditions and estimate stochastic model parameters by allowing for their uncertainty. PCE acts as a post processor of model output and can reduce computation time remarkably compared to other estimation approaches such as the Monte Carlo method or variational approaches. In the present paper, we develop a method to estimate the model parameters of an early diagenesis model by using PCE to estimate both vertical inorganic nitrogen and phosphorus profiles in porewater and release rates of inorganic nitrogen and phosphorus from the sediment.

2. Field data and model

2.1. Target area: Osaka Bay

Osaka Bay, shown in Figure 1, is located in the middle of the main island of Japan and the eastern end of the Seto Inland Sea. The bay is oval, with a length of 60 km, a width of 30 km, and an average depth of 28 m. A strait with a width of 4 km connects Osaka Bay to other areas of the Seto Inland Sea area, and the other with a width of 10 km connects it to the Pacific. It is next to Japan's second largest metropolitan area, which contains Osaka, Kyoto, and Kobe City. Utilization of the coast line as a port started in the twelfth century or earlier, and the shallow area along the northern and eastern shore of the bay has been converted to land used for port facilities, including two airports and industrial and residential areas. Today, the area where the water depth is less than 10 m makes up about 10% of Osaka Bay. The proportion is less than that of other enclosed bays in Japan. Osaka Bay lacks a variety of shallow water areas, that is, a habitat range for benthos and seaweeds has shrunk.

The Yodo River and the Yamato River are the largest and the second largest rivers that flow into the head of the bay. The catchment area of the Yodo River is 8240 km², the amount of total runoff 8458 10⁶ m³, which amounts to a discharge of 267.51 m³ s⁻¹, and the 185-day discharge, which is a daily discharge with a probability of exceedance of about 50%, is 193.47 m³ s⁻¹ (Japan River Association, 2018). This large river discharge contributes to the presence of strong stratification at the head of the bay. Figure 2 shows the isopleths of salinity, the chlorophyll in the surface layer, and dissolved oxygen (DO) in the bottom layer of the port of Osaka (8 km from the Yodo River mouth) and near Kansai Airport (26 km from the Yodo River mouth) in 2012. This shows strong stratification, particularly in the area close to the river mouth in summer, and its influence

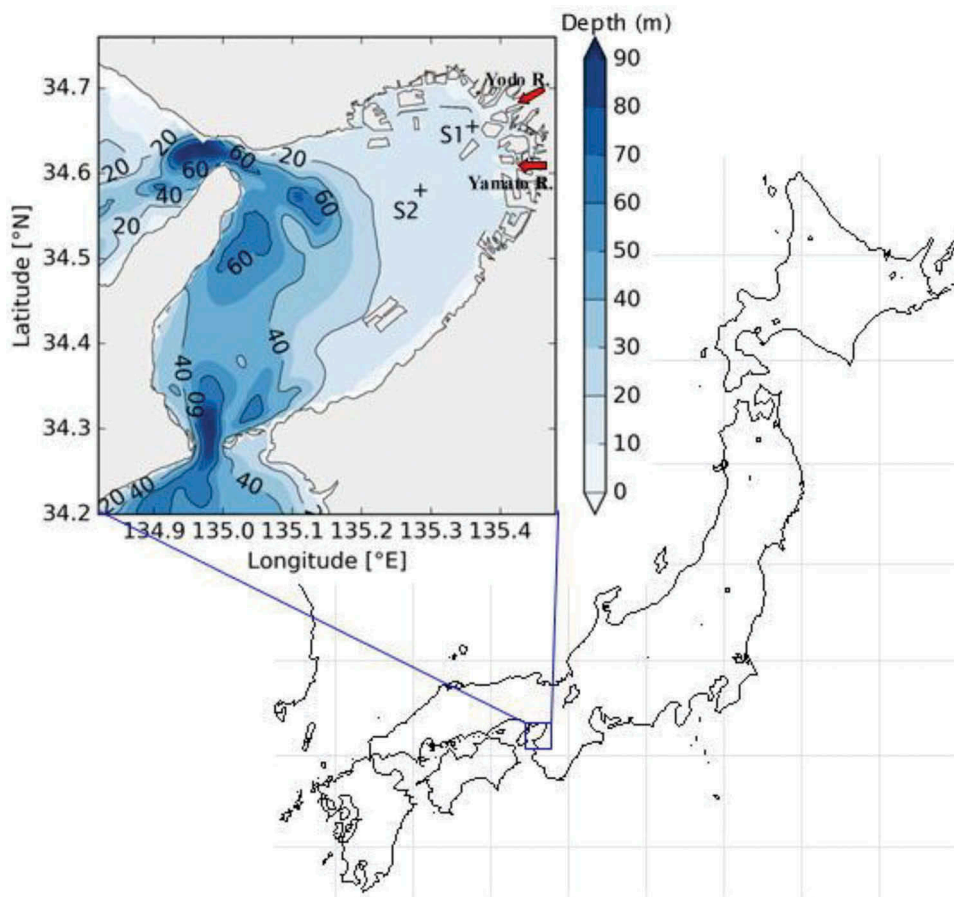


Figure 1. Osaka Bay and a survey site. Plus signs indicate the sampling sites.

on the hypoxia and algae blooming in the river plume and adjacent areas. This estuarine characteristic also produces a density current. Figure 3 shows the residual current system of the bay shown in Nakatsuji and Fujiwara (1997), where the river plume spreads southward and returns northward again. The river plume forms a tidal front along the bathymetry up to a depth of 18–20 m and splits the bay into the eastern and western parts. The compensating bottom current intrudes toward the head of the bay and has a cumulative effect of hypoxic water mass. In the western part, a barotropic flow is dominant and in the eastern part, a baroclinic flow is dominant. Four rivers, including the Yodo and Yamato rivers, deliver more than 70% of the nitrogen and phosphorus from all rivers around the bay (Nakatani, Kawasumi, and Nishida, 2011). This is a cause for the algal blooms occurring annually in spring and autumn. The concentration of chlorophyll reaches a high value greater than $40 \mu\text{g l}^{-1}$ near the river mouth as shown in Figure 2. Nishida, Irie, and Nakatsuji (2006) reveal, from an analysis of the carbon stable isotope in the sediment, that particulate organic matter (POM) derived from land settled down at the bottom of the river channels and “several” (around 5) km from the river mouths. Further, they showed that the POM accumulated in the sediment in the rest of the eastern part of the bay likely

originated from the primary production in the bay. These estuarine characteristics affect the sediment quality. Hypoxia also occurs from early summer to autumn in the eastern area, as shown in Figure 2.

Nakatani (2012) estimated the cycling of nitrogen and phosphorus in Osaka Bay from field surveys, which were carried out on both dry and wet days, and from simulations. Annual total input of inorganic nitrogen was $50.9 \times 10^3 \text{ kg d}^{-1}$ from the outer ocean, $84.5 \times 10^3 \text{ kg d}^{-1}$ from land, and $122.7 \times 10^3 \text{ kg d}^{-1}$ from the bottom sediment. Annual total input of inorganic phosphorus was $7.9 \times 10^3 \text{ kg d}^{-1}$ from the outer ocean, $4.5 \times 10^3 \text{ kg d}^{-1}$ from land, and $22.2 \times 10^3 \text{ kg d}^{-1}$ from the bottom sediment. The release from the bottom is positive in all four seasons. Nishida et al. (2008) reported, from field surveys, that the deposition of nitrogen and phosphorus from air by rain was 3% and 0.4% of their loadings from land. This shows the bottom sediment is a source of nitrogen and phosphorus, and the interaction between the sea water and the sediment has a large impact on the nutrient cycles. Nutrient release rates from the sediment of Osaka Bay which were measured by core sampling and laboratory experiments were reported in several articles. Joh (1986) reported release rates of inorganic nitrogen of $26\text{--}60 \text{ mg m}^{-2} \text{ d}^{-1}$ in a high water-temperature period and $29 \text{ mg m}^{-2} \text{ d}^{-1}$ in a low

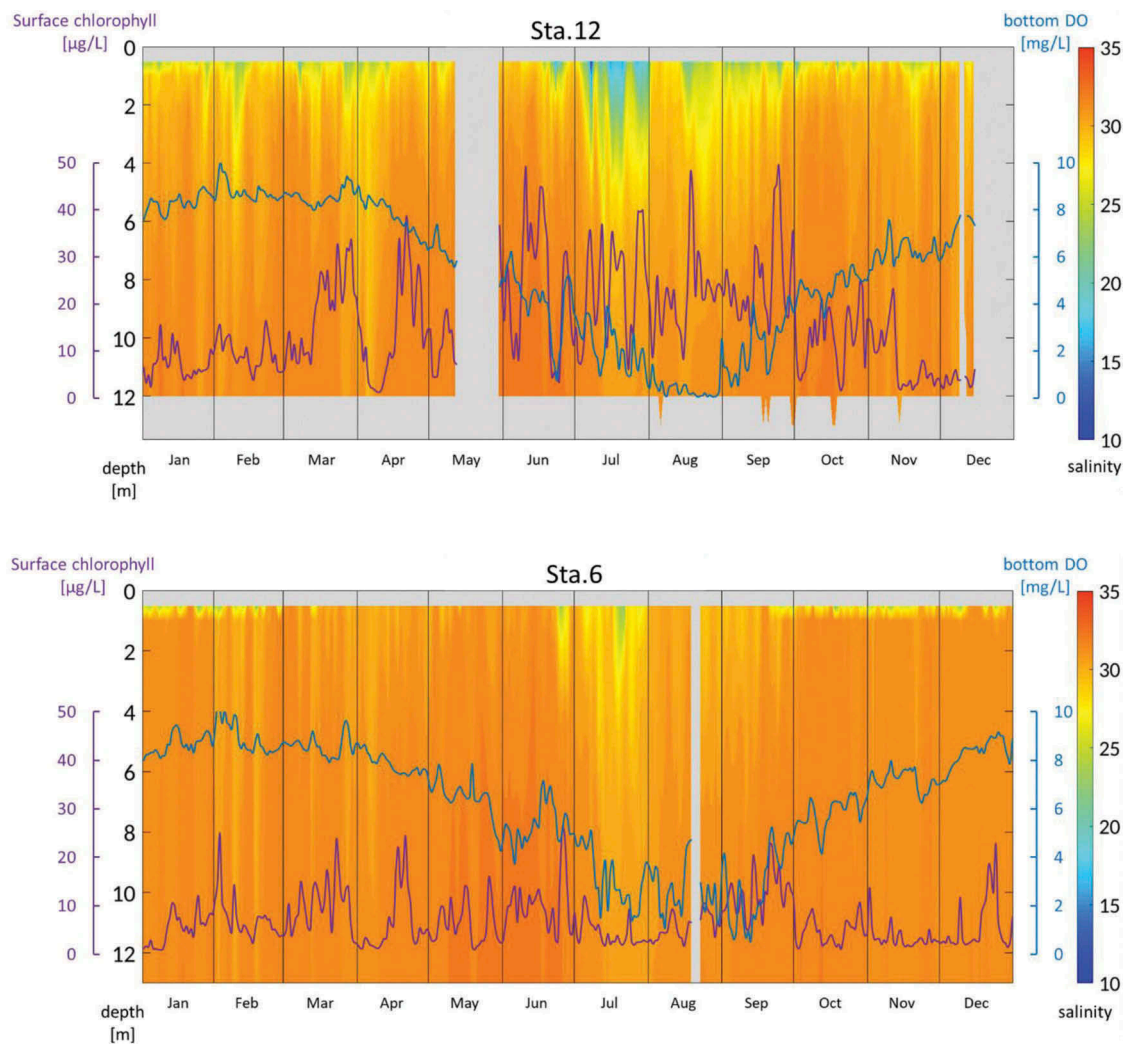


Figure 2. The isopleths of salinity, chlorophyll at the surface, and DO at the bottom (at “Sta. 12”) and at 12 m deep (at “Sta. 6”) in 2012. Station 12 is located in the port of Osaka and Sta. 6 is near Kansai Airport; monitoring was done by Ministry of Land, Infrastructure, Transport and Tourism, Government of Japan (2018).

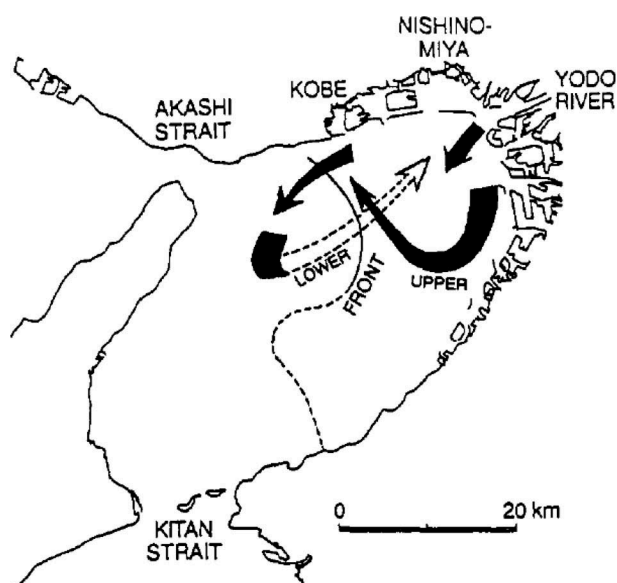


Figure 3. Estuarine vertical circulation in the bay (Nakatsuji and Fujiwara, 1997).

water-temperature period during 1978 at the head of the bay. Han, Nakatsuji, and Nishida (2005)

reported release rates of inorganic nitrogen of 13.2–30.0 $\text{mg m}^{-2} \text{d}^{-1}$ in the eastern part of the bay, 50.7 $\text{mg m}^{-2} \text{d}^{-1}$ in a north innermost port of the head of the bay, and release rates of inorganic phosphorus of 3.7–6.4 $\text{mg m}^{-2} \text{d}^{-1}$ in the eastern part of the bay, 20.1 $\text{mg m}^{-2} \text{d}^{-1}$ in a northern innermost port of the head of the bay in 1999. Irie, Nakatsuji, and Teranaka (2007) reported that in and around depressions due to sand dredging for the past land reclamation in a port of the eastern part, the rates of inorganic nitrogen release were much higher with 136–167 $\text{mg m}^{-2} \text{d}^{-1}$ outside of the dredged area and 223–1164 $\text{mg m}^{-2} \text{d}^{-1}$ in the dredged area, and those of inorganic phosphorus were 3.2–12.7 $\text{mg m}^{-2} \text{d}^{-1}$ outside of the dredged area and 9.6–58.9 $\text{mg m}^{-2} \text{d}^{-1}$ in the dredged area in September 2006. Irie et al. (2011) reported release rates of inorganic nitrogen and phosphorus of 176–341 $\text{mg m}^{-2} \text{d}^{-1}$ and 37–81 $\text{mg m}^{-2} \text{d}^{-1}$, respectively, in front of a sand beach in the northern innermost port. Nakajima, Sano, and Akiyama (2016) reported ammonia release from sediment of -3.22 – $6.86 \text{ mg m}^{-2} \text{d}^{-1}$ in the western

part and 17.50–83.30 mg m⁻² d⁻¹ at the head of the bay. These large variations in nutrient release rates are caused principally by location and survey season but also by a wide variety of sediment characteristics.

2.2. Sampling and laboratory experiment

The vertical profiles of nitrogen and phosphorus in sediments, which are used in this paper, were already reported (Irie et al., 2010), while the release rates of nitrogen and phosphorus from the sediment to the overlying water have not been previously published. Here, we briefly provide an outline of the sampling procedure and laboratory experiments. Undisturbed bottom sediments of about 25 cm thickness and 10.5 cm in diameter were sampled at two sites, Sta. S1 (34° 39' 28" N, 135° 21' 31" E, 12 m deep) and Sta. S2 (34° 35' 05" N, 135° 16' 33" E, 18 m deep) at the head of Osaka Bay, as shown in Figure 1, on October 1, 2009. Please note that the site names are different from those in Irie et al. (2010). On the survey day, DO in the overlying water was not measured due to survey time constraints, but from our other field surveys to clarify the volume of hypoxia, we know that DO in the bottom layer near Sta. S1 was stable since September 24 with a concentration of less than 3 mg l⁻¹. Because the weather in September 2009 was stable with less precipitation than normal, the overlying water remained hypoxic around the survey sites. While the bottom light flux was not measured at the sites, the daily maximum of bottom light flux at the Osaka Port wave observation tower, which is located near Sta. S1 and at which the depth is 12 m, was found to be 2.3 μmol m⁻² s⁻¹ on average during the 2 months from August to September 2010 (instead of that in 2009 because this monitoring has started since 2010). This means that the light was not abundant for most of the microphytobenthos. Core samples were collected by a scuba diver. Three cores were sampled, kept in a bath at the same water temperature as that of the sampling sites during survey and transport to the laboratory, and carried to a laboratory for the measurement of the release rates. Others were separated on boat into the layers of 0–2 cm, 2–5 cm, 5–10 cm, 10–15 cm, 15–20 cm, and 20–25 cm as representatives of the sediment depth of 1, 3.5, 7.5, 12.5, 17.5, and 22.5 cm. These depths and the number of samples were determined according to the limitations of the laboratory equipment and the volume required for chemical analysis and for comparison with previous studies, such as that by Han, Nakatsuji, and Nishida (2005). The samples were kept in coolers with ice during the survey and the transport. They were separated into soil particles and porewater by a centrifuge at 3000 rpm for 20 min. Due to the limitations of the laboratory equipment, we were unable to prevent oxidation during centrifugation. To clarify the characteristics of the sediment, various dissolved and particulate matter fractions were analyzed. Of these, only

ammonia–nitrogen (NH₄–N) and phosphate–phosphorus (PO₄–P) in the porewater are used for the model optimization scheme in this paper. They were analyzed by JIS K0102 42.2 (indophenol blue absorptiometry) and JIS K0102 46.1.1 (molybdenum blue absorptiometry) methods after filtration with 0.2 μm membrane filters (Japanese Industrial Standards Committee, 2016).

To determine the release rates of NH₄–N and PO₄–P, the undisturbed sediment cores with a thickness of about 25 cm in 50 cm pipes were tested in a bath at 25°C in which the water temperature was maintained to that of the sampling sites. Because the DO was not controlled to maintain the ecosystem at the sediment surface, DO decreased throughout the experiment. The overlying water was not displaced and directly used without filtration. Fifty milliliter was sampled 0, 6, 12, 24, 48, and 72 h after the start of the test. The water was not continuously stirred during the incubation. It was stirred two to three times by a glass rod carefully only before sampling of the water. Immediately after sampling, the samples were filtrated through a 1 μm filter and analyzed by a water quality auto analyzer (BI-tec, SWAAT). The release rates were determined based on the difference between the concentration in the water sample overlying the sediment and that in the sea water sample without sediment (the control). The survey required entire daytime hours, and a few hours were spent in transportation. All laboratory analyses started in the evening of the survey day.

Irie et al. (2010) sampled four sites, although only the data from two of those sites are used here. The other sites were located in a port of the northern innermost area (Sta. P1, "S1" in Irie et al. (2010)) and in the west of the targeted sites, where the depth is greater (Sta. S4 in Irie et al. (2010)). The release rates of NH₄–N and PO₄–P at Sta. P1 were 74.1 and 8.3 mg m⁻² d⁻¹, respectively. The ratio of these release rates at Sta. P1 is higher than those at Sta. S1 and S2. Because of this difference, the modeling with the PCE technique could not obtain presumable parameter values. At Sta. S4, the relationship between the release rates and the vertical profiles in the sediment is unclear. Sta. S4 is located outside the river plume. In recent years, the concentration of nutrients in the Seto Inland Sea has become lower than those in the past few decades. This long-time trend could start changing the dynamics of nutrient release and the relationship between the release and the accumulated organic matter. At Sta. 4, in the following surveys in 2011, a large amount of benthos can be seen in sample cores. The early diagenesis model used here considers only the physical processes of benthos, that is, bioturbation and bioirrigation, and does not take account of the biological processes. This uncertainty and the unclear long-year trend are possible causes that decrease model skill. We do not have a clear answer for why the scheme used in this study could not work well at Sta. S4. Irie et al. (2010) mainly focused on the impact of hydrogen sulfide release on the expansion of hypoxia using the connected

models. The model showed the role of hydrogen sulfide release qualitatively, although the total sediment oxygen consumption could not be simulated quantitatively. This fact is a motivation for developing a scheme to find parameter values that can reproduce sediment profiles and the release rates simultaneously.

2.3. Early diagenesis model

In the present study, a one-dimensional (1D) vertical sediment model known as an early diagenesis model was constructed based on the research by Fossing et al. (2004) and Kasih et al. (2009) and used to account for the biochemical interactions between the various substances contained in sediment particles and porewater. Pioneering research of an early diagenesis model was conducted by Berner (1964) who developed a model for the dynamics of sulfur in surface sediment. This early stage of the model development work was summarized in Berner (1980). Numerous pieces of subsequent model development have occurred in the past 50 years are reviewed in many articles such as Berner (1974), Van der Weijden (1992), and Boudreau (1997). In one of the latest reviews, Arndt et al. (2013) categorize the various sediment models. For example, Boudreau (1996), Van Cappellen and Wang (1995,

1996), Boudreau (1996), and Wang and van Cappellen (1996) include the description of iron and sulfur cycling and are governed by the conservation of alkalinity in porewater. In contrast, Soetaert, Herman, and Middelburg (1996a, 1996b) constructed a model that mainly simulates the cycling of carbon and nitrogen. Soetaert's model focused on the remineralization processes of organic matter under anaerobic condition but treated them as a single process. Wijsman et al. (2002) improved Soetaert's model by resolving the individual mineralization processes. Berg, Rysgaard, and Thamdrup (2003) also introduced detailed descriptions of transport contributions by bioturbation, bioirrigation, and additional processes. Fossing et al. (2004) extended the model of Wijsman to the cycling of phosphorus. In the Wijsman–Fossing type model pH is just a parameter and not conserved. Kasih et al. (2009) regarded the organic matter settling down from the overlying water as particulate organic matter and considered time for hydrolyzation in the sediment. A schematic of this model based on the model of Kasih and implemented in this paper is shown in Figure 4. Table 1 shows state variables of dissolved and solid species included in the model. The model is fundamentally based on an advection (burial)-diffusion-reaction equation (Berner, 1980; Boudreau, 1997):

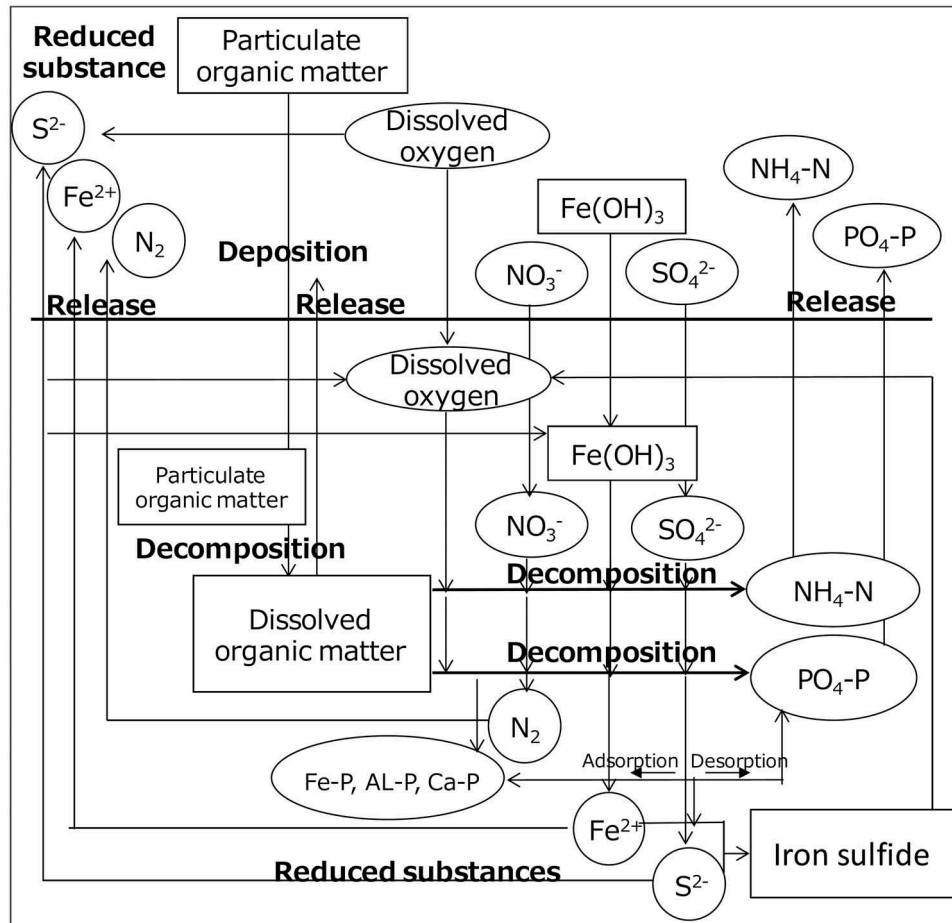


Figure 4. Schematic of early diagenesis model in this study.

Table 1. Solute and solid species included in the model.

Solute state variables	Solid-state variables
($\mu\text{mol l}^{-1}$)	($\mu\text{mol dm}^{-3}$)
DOMf	POMf
DOMs	POMs
O ₂	POMn
NO ₃ ⁻	MnO ₂
SO ₄ ²⁻	Fe(OH) ₃
NH ₄ ⁺	FeS
Mn ²⁺	FeS ₂
Fe ²⁺	
ΣH ₂ S	
CH ₄	
PO ₄ ³⁻	

$$\begin{aligned}
& [\Phi + \rho_s(1 - \Phi)K'] \frac{\partial C}{\partial t} \\
& = \frac{\partial}{\partial z} \left\{ [\Phi(D_{Bw} + D_s) + \rho_s(1 - \Phi)D_{Bs}K'] \frac{\partial C}{\partial z} \right\} \\
& - \frac{\partial}{\partial z} \{ [\Phi w_x + \rho_s(1 - \Phi)w_zK'] C \} \\
& + \Phi\alpha(C_o - C) + R \quad (1)
\end{aligned}$$

where Φ is porosity, ρ_s is density of sediment, K' is an adsorption constant, C is the concentration of the substances, t is time, z is depth from the surface of sediment, D_s is sediment diffusivity, D_{Bw} and D_{Bs} are biodiffusion coefficients of dissolved and solid substances, w_x and w_z are burial rates of dissolved and solid substances, α is the bioirrigation parameter, C_o is the concentration of the substances in overlying bottom water, and R is the reaction term. Detailed descriptions of this type of model are introduced by Fossing et al. (2004) and Kasih et al. (2009). This model neither considers the influence of shear stress and flow velocity on boundary layer nor the resuspension by wind.

Table 2 shows major reactions in the model and Table 3 presents model parameters. The first aspect of this model is the deposition of POM, which is hydrolyzed into dissolved organic matter (DOM). Under aerobic conditions, this organic matter is mineralized using DO. However, under anaerobic conditions, other oxides are used in the primary reaction: first nitrate ions, then manganese and iron ions, and finally sulfate ions. During this process, intermediates such as inorganic nitrogen and phosphorus, and reduced substances are also produced. Biochemical secondary reactions occur through these intermediate products. The 1D model was constructed to resolve processes vertically to a depth of 16 cm into the sediment, and was partitioned into a total of 40 layers. To more clearly capture the phenomena occurring at the surface of the sediment, where vigorous reactions occur, the layers were decreased in size closer to the surface. The surface layer is thinnest at 0.02 cm and the lowest layer is thickest at 0.8 cm. The time step was set to 1 min, and 1 year was taken to be 365 days. To consider the effect of seasonal variation, the temperature of the water overlying the sediment, DO concentration, and POM flux

Table 2. Primary (mineralization) and secondary reactions in the model (Kasih et al., 2009).

Decomposition of POM	
POMf → DOMf + DOMs	
POMs → DOMf + DOMs	
Primary reactions	
O ₂ + DOM (f,s) → CO ₂ + H ₂ O	R1
4NO ₃ ⁻ + DOM (f,s) + 4H ⁺ → N ₂ + 5CO ₂ + 7H ₂ O	R2
2MnO ₂ + DOM (f,s) + 4H ⁺ → 2Mn ²⁺ + CO ₂ + 3H ₂ O	R3
4FeOOH + DOM (f,s) + 8H ⁺ → 4Fe ²⁺ + CO ₂ + 7H ₂ O	R4
SO ₄ ²⁻ + DOM (f,s) + 2H ⁺ → H ₂ S + 2CO ₂ + 2H ₂ O	R5
Secondary reactions	
NH ₄ ⁺ + 2O ₂ → NO ₃ ⁻ + H ₂ O + 2H ⁺	R6
FeOOH + PO ₄ ³⁻ → FeOOH≡ PO ₄ ³⁻	R7
2Fe ²⁺ + MnO ₂ + H ₂ O → 2FeOOH + Mn ²⁺ + 2H ⁺	R8
2Mn ²⁺ + O ₂ + 2H ₂ O → 4MnO ₂ + 4H ⁺	R9
H ₂ S + 2FeOOH≡ PO ₄ ³⁻ + 4H ⁺ → S ⁰ + 2Fe ²⁺ + 4H ₂ O + 2PO ₄ ³⁻	R10a
4Fe ²⁺ + O ₂ + 6H ₂ O → 4FeOOH + 8H ⁺	R11
H ₂ S + 2FeOOH + 4H ⁺ → S ⁰ + 2Fe ²⁺ + 4H ₂ O	R10b
H ₂ S + MnO ₂ + 2H ⁺ → S ⁰ + Mn ²⁺ + 2H ₂ O	R12
H ₂ S + Fe ²⁺ → FeS + 2H ⁺	R13
FeS + S ⁰ → FeS ₂	R14
SO ₄ ²⁻ + 3H ₂ S + 4FeS + 2H ⁺ → FeS ₂ + 4H ₂ O	R15
H ₂ S + 2O ₂ → SO ₄ ²⁻ + 2H ⁺	R16
FeS + 2O ₂ → Fe ²⁺ + SO ₄ ²⁻	R17
2FeS ₂ + 7O ₂ + 2H ₂ O → 2Fe ²⁺ + 4SO ₄ ²⁻ + 4H ⁺	R18
4S ⁰ + 4H ₂ O → 3H ₂ S + SO ₄ ²⁻ + 2H ⁺	R19
MnO _{2A} → MnO _{2B}	R20
FeOOH _A → FeOOH _B	R21

were given a sine function with a period of 1 year. Additionally, to obtain a stable initial vertical distribution, a model spinup of 200 years was run. Next, the values for the parameters were changed, and simulations were conducted for a 100-year period.

2.4. Parameter estimation using polynomial chaos expansion

In the present study, an emulator technique called PCE is used to accelerate parameter estimation. Emulators can provide accurate approximations of numerical model outputs based on existing model results. Emulators can thus be used to propagate adjustments in the model inputs, such as model parameters, boundary conditions, and external forcing, to the model output, without the requirement for additional model evaluations. This approach speeds up procedures that rely on repeated model evaluations like parameter estimation experiments. PCE has been widely used in engineering applications; for an overview, see Xiu and Karniadakis (2003) and references therein. Examples of the use of the PCE in parameter estimation in the context of biological ocean models are the studies by Mattern, Fennel, and Dowd (2012, 2013). In contrast to previous studies, we apply PCE to an early diagenesis model: in this study PCE is used to estimate the values of two model parameters simultaneously. The simultaneous estimation can be performed effectively because PCE only requires a small number of model evaluations for two parameters (in our PCE implementation: 25 simulations) which are used to approximate the model output for arbitrary values of the two parameters. The PCE approximation is based on polynomial interpolation:

Table 3. Model parameters in this study. Subscript number of K indicates a rate constant for the number of reaction shown in Table 2.

Model parameter	Value	Unit	Values in references
Reaction rate constants			
KPOM _f	2.5 10 ⁻⁶	s ⁻¹	(F)9.610 ⁻⁶ (K)2.5 10 ⁻⁶ (B)2.4 10 ⁻⁶
KPOM _s	6.0 10 ⁻¹⁰	s ⁻¹	(F)1.210 ⁻⁸ (K)1.2 10 ⁻¹⁰ (B)3.0 10 ⁻⁹
KDOM _f	1.0 10 ⁻³	s ⁻¹	(K)1.0 10 ⁻³
KDOM _s	5.0 10 ⁻⁸	s ⁻¹	(K)5.0 10 ⁻⁹
K6	2.5 10 ⁻⁷	μM ⁻¹ ·s ⁻¹	(F)2.510 ⁻⁶ (K)(B)2.5 10 ⁻⁷
K7	5.0 10 ⁻¹⁴	s ⁻¹	(F)5.010 ⁻¹¹ (K)5.0 10 ⁻¹⁴
K8	1.7 10 ⁻⁹	μM ⁻¹ ·s ⁻¹	(F)1.710 ⁻⁸ (K)1.7 10 ⁻⁹
K9	1.5 10 ⁻⁵	μM ⁻¹ ·s ⁻¹	(F)(K)1.5 10 ⁻⁵
K10	2.0 10 ⁻⁷	μM ⁻¹ ·s ⁻¹	(F)2.010 ⁻⁸ (K)2.0 10 ⁻⁷
K11	5.0 10 ⁻⁴	μM ⁻¹ ·s ⁻¹	(F)(K)5.0 10 ⁻⁴
K12	3.0 10 ⁻⁹	μM ⁻¹ ·s ⁻¹	(F)(K)3.0 10 ⁻⁹
K13	3.75 10 ⁻⁵	μM ⁻¹ ·s ⁻¹	(F)7.510 ⁻⁷ (K)3.75 10 ⁻⁵
K14	3.0 10 ⁻¹⁰	cm ³ ·nmol ⁻¹ ·s ⁻¹	(F)3.010 ⁻¹² (K)3.0 10 ⁻¹⁰
K15	7.5 10 ⁻¹²	s ⁻¹	(F)2.510 ⁻¹¹ (K)7.5 10 ⁻¹²
K16	5.0 10 ⁻⁵	μM ⁻¹ ·s ⁻¹	(F)(K)5.0 10 ⁻⁵
K17	6.0 10 ⁻⁷	μM ⁻¹ ·s ⁻¹	(F)(K)6.0 10 ⁻⁷
K18	3.0 10 ⁻¹⁰	μM ⁻¹ ·s ⁻¹	(F)1.610 ⁻⁸ (K)(B)3.0 10 ⁻¹⁰
K19	7.0 10 ⁻⁷	s ⁻¹	(F)(K)7.0 10 ⁻⁷
K20	1.3 10 ⁻⁹	s ⁻¹	(F)(K)1.3 10 ⁻⁹
K21	9.0 10 ⁻¹⁰	s ⁻¹	(F)(K)9.0 10 ⁻¹⁰
Constituent ratios			
FPOMn/FPOM _{total}	0.20		(F)0.08 (K)0.2
FPOMf/FPOM _{total}	0.57		(F)0.42 (K)0.4
FFeOOHA/FFeOOHB	0.50		(K)0.5
C/N	10		(F)10 (K)8
C/P	70		(F)80 (K)70
DOMf/DOM _{total}	0.50		(K)0.75
Limiting concentrations			
O ₂ limit	20	μM	(F)(K)20
NO ₃ limit	5	μM	(F)(K)5
MnO ₂ limit	5.0 10 ⁴	nmol g ⁻¹	(F)(K)50,000
FeOOHlimit	1.0 10 ⁵	nmol g ⁻¹	(F)(K)100,000
Inhibiting H₂S concentrations in sulfide hydrolysis reaction			
H ₂ S _{stop}	10	μM	(F)(K)10
Bioirrigation rates			
a_irr	0.885		(F)0.885
b_irr	0.054		(F)0.054
c_irr	2.53		(F)2.53
d_irr	0.352		(F)0.352
e_irr	6.00		(K)6
f_irr	0.05		(K)0.05
Biodiffusivity of solutes			
DB _w (z ≤ 11.8 cm)	3.51 10 ⁻⁶	cm ² s ⁻¹	(F)3.51 10 ⁻⁶ (K)8 · e ^(-0.4z)
DB _w (z > 11.8 cm)	3.51 10 ⁻⁶ e ^{-0.378(z-11.8)}	cm ² s ⁻¹	(F)3.51 10 ⁻⁶ e ^{-0.378(z-11.8)} (K)8 · DB/10
Biodiffusivity of solids			
DBs	DB/9.3	cm ² s ⁻¹	(K)DB/9.3
Adsorption constants			
KdNH ₄	1.5	cm ³ ·g ⁻¹	(F)2.2 (K)1.5
KdNO ₃	5.4	cm ³ ·g ⁻¹	(K)5.4
KdMn	13.0	cm ³ ·g ⁻¹	(F)(K)13.0
KdFe	500	cm ³ ·g ⁻¹	(F)(K)500
KdPO ₄	2.0	cm ³ ·g ⁻¹	(F)(K)2.0

(F)Fossing et al. (2004); (K)Kasih et al. (2009); (B)Berg, Rysgaard, and Thamdrup (2003); (W)Wijnsman et al. (2002)

$$f(\theta) = \sum_{k=0}^{k_{\max}} a_k \Phi_k(\theta) + \varepsilon_{trunc}(\theta) \quad (2)$$

where $\theta = (\theta_1, \theta_2)^T$ is the parameter with uncertainty, $f(\theta)$ is the approximate output of the model for parameter values θ , a_k are coefficients that need to be computed, $\Phi_k(\theta)$ are polynomials of order k , k_{\max} is the highest order of polynomials considered in the approximation. The polynomials used in the PCE approximation are orthogonal to each other with respect to the distribution of θ which needs to be specified a priori. Following Mattern, Fennel, and Dowd (2012), we select uniform distributions for θ_1 and θ_2 . This choice requires $\Phi_k(\theta)$ to be Legendre polynomials (for details including a list of distributions

and associated polynomials, see Xiu and Karniadakis (2002)). A higher value of k_{\max} in Equation (2) reduces the truncation error $\varepsilon_{trunc}(\theta)$, but increases the computational cost of the approximation, because the calculation of a_k for $k = 0 - k_{\max}$ requires $k_{\max} + 1$ model evaluations. In our application, k_{\max} is set to 4, requiring five model evaluations for each parameter, resulting in $5 \times 5 = 25$ total simulations for any two parameters estimated simultaneously.

To optimize the parameters, we estimated the parameter values that could minimize the misfit between the approximate model results $f(\theta)$ and observed values. The observed values used for the optimization were the pore-water concentrations of NH₄-N and PO₄-P and the release rates obtained from the results of a survey

conducted on October 1, 2009. Because different units were used for the release rates and the concentrations in porewater, there were large differences in the $\text{NH}_4\text{-N}$ and $\text{PO}_4\text{-P}$ values and in their vertical profiles in porewater; consequently useful results could not be obtained using a simple root mean square error (RMSE) to qualify model-observation difference. Thus, as results of testing some evaluation functions, we chose the evaluations using a dimensionless RMSE (Dist) equation, as shown below, which easily reproduced the vertical profile in porewater:

$$\text{Dist} = \sqrt{\frac{\sum_{n=1}^{12} [(obs_n - cal_n)/(obs_n + cal_n)]^2}{12}} \quad (3)$$

where *obs* is an observation and experimental value and *cal* is a model result. The number 12 corresponds to the evaluation of a total of six variables, which included the $\text{NH}_4\text{-N}$ and $\text{PO}_4\text{-P}$ porewater concentrations at five depths in the sediment and the release rates for both $\text{NH}_4\text{-N}$ and $\text{PO}_4\text{-P}$. Using this evaluation equation, it was possible to avoid overestimating the misfit at a layer for which a concentration of almost zero was observed, compared to other layers, because the misfit between the calculated and observed values for that layer was divided by a number close to zero.

As a result of sensitivity analysis, when there are more than two parameters that should be optimized, we optimize two parameters at a time and sequentially go through other parameters. The first two parameters are optimized and then the values are set and used in the next estimation experiment. Sequential order of parameters is adjusted by trial basis and empirically.

2.5. Other model settings

To keep the model parameters to be estimated by PCE at minimum, sensitivity analyses are performed preliminarily. In both simulations using the early diagenesis model, boundary conditions and other settings were identical. The concentration of DO in overlying water and POM flux has seasonal variation defined with a sine curve. The concentrations of other material in the overlying water is constant, 0.02 mg l^{-1} for $\text{NH}_4\text{-N}$, 0.02 mg l^{-1} for $\text{NO}_3\text{-N}$, 0.01 mg l^{-1} for $\text{PO}_4\text{-P}$, and 0 mg l^{-1} for $\Sigma\text{H}_2\text{S}$. Porosity in the surface sediment is 0.88. Burial rate in the surface layer is $0.38 \text{ cm year}^{-1}$. Both porosity and burial rates decrease toward the deeper sediment layers.

3. Sensitivity analysis

The model used in this study has many parameters, including the rate constant for the decomposition process and the organic matter ratio. Sensitivity analyses were conducted to determine the parameters to be estimated from these. Of the results calculated with

the early diagenesis model, the porewater concentrations of $\text{NH}_4\text{-N}$ and $\text{PO}_4\text{-P}$ and the release rates of $\text{NH}_4\text{-N}$ and $\text{PO}_4\text{-P}$ were used to investigate the sensitivity of the model to the parameters. Although the parameter values differ from those of prior research, "default" values are required when conducting the sensitivity analysis. These values are listed in Table 3.

The results of the sensitivity analyses show that although some parameters have little effect on the concentrations in porewater, other parameters have a large influence on it. In particular, changes in the rate constant of the primary reaction system and parameters that reflect the composition ratios of organic matter have large impacts on the vertical profiles of $\text{NH}_4\text{-N}$ and $\text{PO}_4\text{-P}$ in the porewater. In this paper, we present four examples that include parameters that have large or little influence.

To determine the degradation rate constant of slowly degradable particulate organic matter (KPOM_s), simulations were conducted with values of 1/50, 1/10, 10, and 50 times of the default KPOM_s value. Based on the results obtained from these, the concentration of $\text{NH}_4\text{-N}$ in porewater is shown in Figure 5. Compared to the results of the simulation with the default KPOM_s , both larger and smaller KPOM_s values exhibit lower concentrations of $\text{NH}_4\text{-N}$ in the porewater. Additionally, the vertical distribution of the amount of slowly degradable POM (POMs) shown in Figure 6 changes by the degradation rate. When the degradation constant is larger than the default, POM rapidly degrades. Moreover, it is likely that the porewater $\text{NH}_4\text{-N}$ concentration is low because there was no POM that could be degraded in most of the deep sediment. In contrast, when the degradation constant is smaller than the default value, there is a large quantity of POMs in most of the deep sediment. Because the amount of degradation is less than the default value, resulting the concentration of $\text{NH}_4\text{-N}$ in the porewater is low.

The changes in the $\text{NH}_4\text{-N}$ concentration in the porewater upon changing the fast-degradable organic matter ratio ($\text{FPOMf}/\text{FPOMtotal}$ (in Table 3), hereafter denoted as "fast/*t*") are shown in Figure 7. There are two parameters related to the organic matter ratios: the fast-degradable organic matter ratio and non-degradable organic matter ratio. The proportion of slowly degradable organic matter could be determined by subtracting the fast-degradable organic matter and non-degradable organic matter from the total organic matter. If there is a large proportion of fast-degradable organic matter, the $\text{NH}_4\text{-N}$ concentration in the porewater decreases with the exception of the uppermost surface layers. Since the deposition continues slowly, surface sediment takes a long time, on the order of several decades, to reach the lower layers. Because the amount of slowly degradable organic matter is greater for smaller proportions of fast-degradable organic matter, the $\text{NH}_4\text{-N}$ concentrations in the porewater increase in the lower layers.

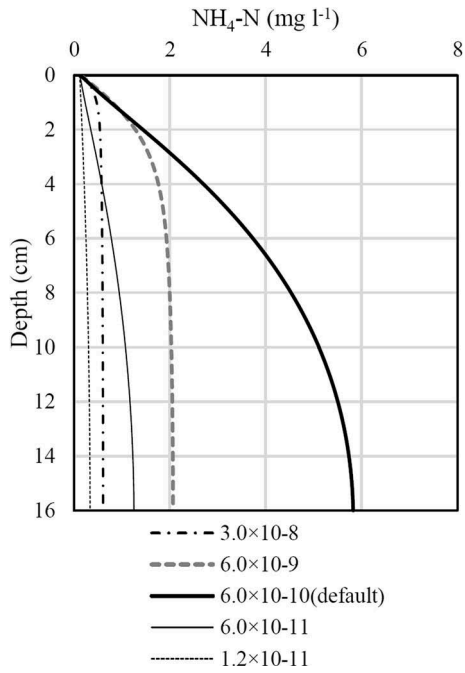


Figure 5. Influence of degradation rate constant of slowly degradable particulate organic matter (KPOM_s) on vertical profiles of NH₄-N.

The changes in the NH₄-N concentration in porewater upon changing the ratio of carbon and nitrogen (C/N) in the organic matter which newly settles down to the seabed surface are shown in Figure 8. Increasing the C/N ratio causes the porewater NH₄-N concentration to decrease. This is because there is less nitrogen in the organic matter if the C/N ratio is large.

The changes in the NH₄-N concentration in the porewater upon changing the rate constant for the nitrification reaction (K₆), which is one of the secondary reactions, are shown in Figure 9. Because nitrification proceeds when the rate constant is large, the concentration of NH₄-N is lowered in the porewater; however, the change is slight even for a 250-fold change in the reaction rate.

Table 4 shows other results of sensitivity analyses upon changing a model parameter. Dimensionless difference (DD) is defined by the following equation which is a similar index defined by Equation (3):

$$DD = \sqrt{\frac{\sum_{n=1}^{12} [(cal_{50,n} - cal_{1/50,n}) / (cal_{50,n} + cal_{1/50,n})]^2}{12}} \quad (4)$$

where $cal_{50,n}$ and $cal_{1/50,n}$ are the simulated values with the 50 and 1/50 times of the default value, the number 12 means two release rates of NH₄-N and PO₄-P and the NH₄-N and PO₄-P concentrations at five depths, which correspond to the depths where the field samples are analyzed. Only the rate constant for nitrification and the

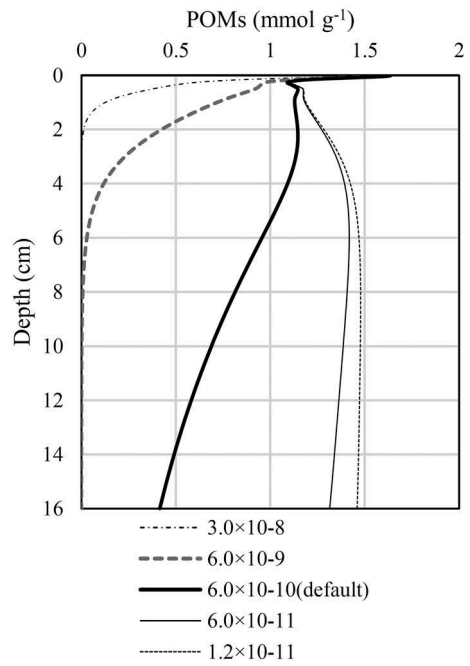


Figure 6. Influence of degradation rate constant of slowly degradable particulate organic matter on vertical profiles of POMs (slowly degradable particulate organic matter).

ratios for fractionation have a large impact on the vertical profiles of porewater concentrations. Based on the results of the sensitivity analyses, six parameters were used for the parameter estimation: the degradation rate constant for fast-degradable DOM in dissolved organic matter (K_{DOM_f}), degradation rate constant for slowly degradable particulate organic matter (KPOM_s), fast-degradable organic matter ratio to total organic matter (fast/t), non-degradable organic matter ratio to total organic matter

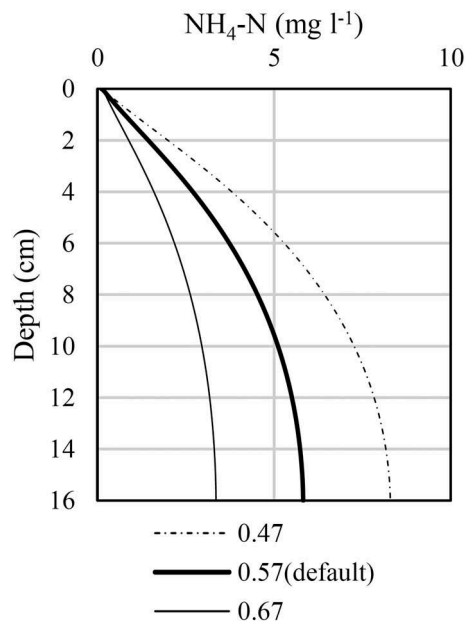


Figure 7. Influence of the fast-degradable organic matter ratio on vertical profiles of NH₄-N.

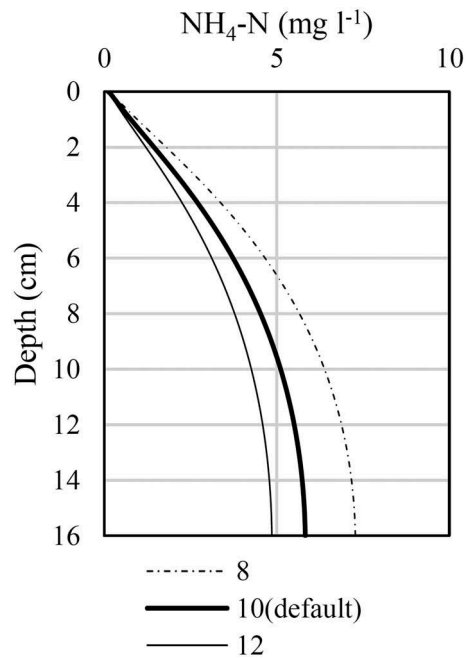


Figure 8. Influence of C/N ratio on vertical profiles of $\text{NH}_4\text{-N}$.

(non/t), C/N ratio of the organic matter, and C/P ratio of the organic matter.

4. Estimation results and discussion

Because each parameter can have a wide range, two parameters are estimated simultaneously by the PCE. Estimation is first performed for KDOM_f and non/t (Case 1). The contour map of the evaluation index Dist for Case 1 is shown in Figure 10. As prior distributions for all parameters that considered in this study, uniform distribution is used, because we cannot have enough data for using a normal distribution. The lower and upper limits for KDOM_f and non/t are 1.0×10^{-2} to 5.0×10^{-1} and 0–0.5, respectively. Multicolor lines indicate isopleths of Dist. The 25 black crosses are the values of the parameter set for which model simulations were performed, and the blue cross shows the optimum parameter values that minimize Dist. The porewater concentrations and release rates of $\text{NH}_4\text{-N}$ and $\text{PO}_4\text{-P}$ for the results obtained from the simulation with the default values

Table 4. Dimensionless difference of porewater concentrations by parameter values.

Parameter	Difference	Parameter	Difference
KDOM_f	4.23 E^{-2}	K12	$<1.0 \text{ E}^{-8}$
KDOM_s	1.25 E^{-3}	K13	$<1.0 \text{ E}^{-8}$
KPOM_f	9.35 E^{-3}	K14	$<1.0 \text{ E}^{-8}$
KPOM_s	6.43 E^{-2}	K15	$<1.0 \text{ E}^{-8}$
K6	2.42 E^{-5}	K16	7.41 E^{-7}
K7	$<1.0 \text{ E}^{-8}$	K17	$<1.0 \text{ E}^{-8}$
K8	$<1.0 \text{ E}^{-8}$	K18	$<1.0 \text{ E}^{-8}$
K9	$<1.0 \text{ E}^{-8}$	K19	$<1.0 \text{ E}^{-8}$
K10	$<1.0 \text{ E}^{-8}$	K20	$<1.0 \text{ E}^{-8}$
K11	$<1.0 \text{ E}^{-8}$	K21	$<1.0 \text{ E}^{-8}$

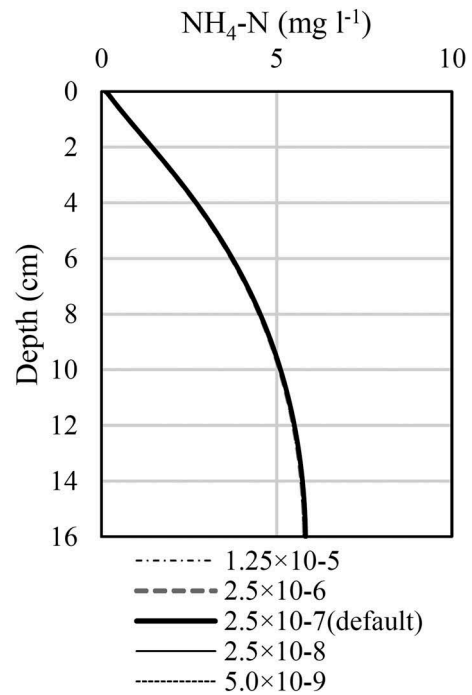


Figure 9. Influence of rate constant for the nitrification reaction (K6) on vertical profiles of $\text{NH}_4\text{-N}$.

and the results of a simulation using Case 1 are shown in Figures 11 and 12, respectively. In the simulations using the default values, neither the porewater concentrations nor the release rates of $\text{NH}_4\text{-N}$ and $\text{PO}_4\text{-P}$ sufficiently reproduced the measured values and experimental results. Although the observed porewater concentrations of $\text{NH}_4\text{-N}$ are reproduced well for the layers near the surface when the parameter values estimated by Case 1 are used, large differences from the measured values still appear in the deep layers. The experimental result for the release rate was $70.3 \text{ mg m}^{-2} \text{ d}^{-1}$, which was well reproduced by the calculated value of $61.6 \text{ mg m}^{-2} \text{ d}^{-1}$ when the optimal value set is used. Similar trends are also found for the release of $\text{PO}_4\text{-P}$.

Next, KPOM_s and fast/t were estimated with the optimal KDOM_f and non/t which were estimated in Case 1 and the other default values. The estimation result is denoted as Case 2. The lower and upper limits for KPOM_s and fast/t are 1.0×10^{-9} – 1.0×10^{-8} and 0–1, respectively in Case 2. Additionally, because there was considerable uncertainty in the degradation rate constant and organic matter ratio, another estimation (Case 3) was conducted with a simulation limits of 0.7–1.3 times of estimated results in Cases 1 and 2 as references. Finally, using Case 3, the C/N and C/P ratios of the organic matter were estimated (Case 4). The parameter values obtained from these several instances of estimation are listed in Table 5. The porewater concentrations of $\text{NH}_4\text{-N}$ and $\text{PO}_4\text{-P}$ resulting from these values are shown in Figure 13, and the release rates of $\text{NH}_4\text{-N}$ and $\text{PO}_4\text{-P}$ are shown in Figure 14. These figures show that the reproducibility of the porewater concentrations

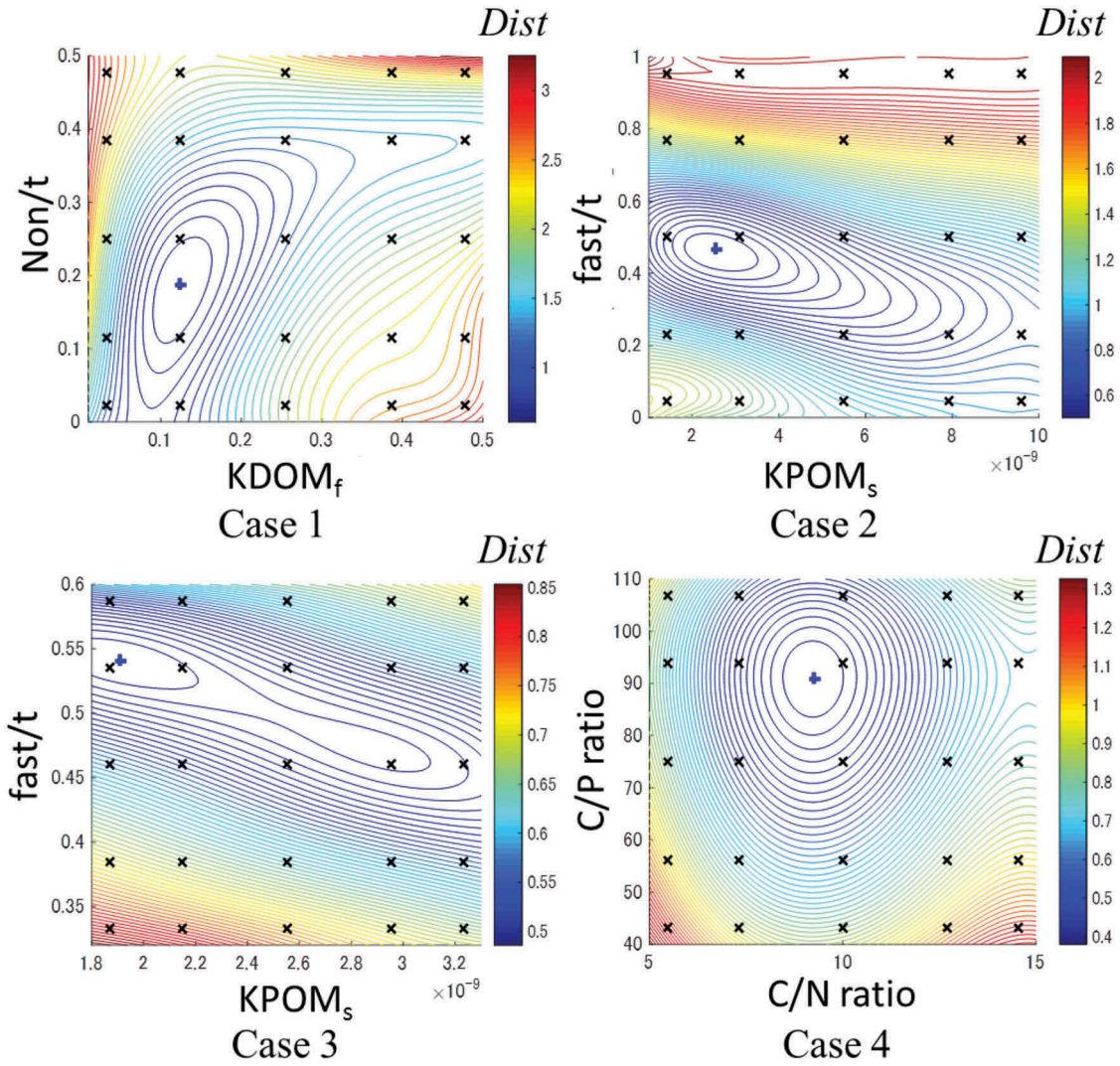


Figure 10. Distributions of Dist for $KDOM_f$ and non/t (Case 1), $KPOM_s$ and fast/t (Case 2), $KPOM_s$ and fast/t (Case 3), and C/N ratio and C/P ratio (Case 4).

and release rates gradually increases with those sequential parameter estimations. Especially, in Case 4, the estimated C/P ratio improves the simulation of the

release rate of PO_4-P well in exchange of the slightly less reproducibility of the PO_4-P vertical profiles.

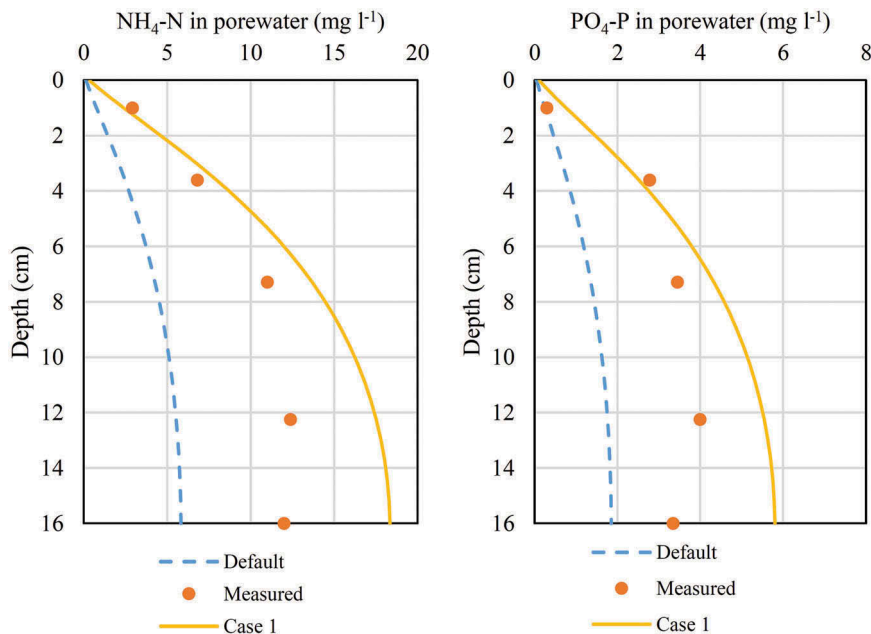


Figure 11. Porewater concentrations of NH_4-N (left) and PO_4-P (right).

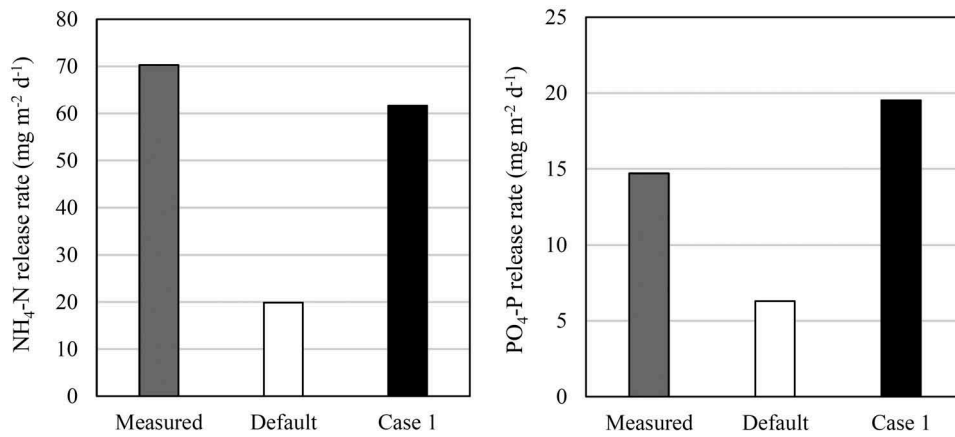


Figure 12. Release rates of NH₄-N (left) and PO₄-P (right).

As a result of using the PCE method to estimate six parameters, it was possible to obtain well-reproduced porewater concentrations and release rates of NH₄-N and PO₄-P, and obtain the optimum parameters for representing the state of the sediment at the times and locations of the observations.

The above procedure proposed in this study is summarized in Figure 15 as a diagram. Using the same procedure, parameter estimation with the data sampled at Sta. S1 is carried out (Figure 16). Table 6 shows the estimated parameter values. The estimated C/N ratios of POM settling down to the bed at Sta. S1 and Sta. S2 are 9.9 and 9.2, respectively. The ratio is 40–50 % higher than the Redfield ratio of 106:16 and almost corresponds to the C/N ratio of fast-degradable DOM of 9.95 reported by Hopkinson and Vallino (2005). It is in the range of the globally varied C/N ratio of POM and higher than the average shown in Martiny et al. (2013). The estimated C/P ratios of POM at Sta. S1 and S2 are 82.6 and 90.9, and these values are higher than the default value (Kasih et al., 2009) and the ratio

of 80 set up in the model in Fossing et al. (2004). The ratio is, however, lower than well-known range of C/P ratio; Redfield ratio of 106:1, 78–195 for POM in Martiny et al. (2013), 400 for prokaryotes in marine sediment in Steenbergh et al. (2013). Okaichi (1979) reported that C/N/P was 110:16:2 for phytoplankton and 158:17:1 for detritus of the western Seto Inland Sea, because phytoplankton stored phosphorus excessively. Ratios that reflect a higher C/N ratio and lower C/P ratio than the conventional Redfield ratio and those values shown in the latest research works are a cause of the difficulty in modeling the material cycles in marine sediment and estimating the flux of inorganic nitrogen and phos-

Table 5. Results of estimated parameters at Sta. S2.

	Case 1	Case 2	Case 3	Case 4
KDOM _f	1.2×10^{-1}	1.2×10^{-1}	9.4×10^{-2}	9.4×10^{-2}
non/t	0.19	0.19	0.16	0.16
KPOM _s		2.5×10^{-9}	1.9×10^{-9}	1.9×10^{-9}
fast/t		0.46	0.54	0.54
C/N ratio				9.2
C/P ratio				90.9

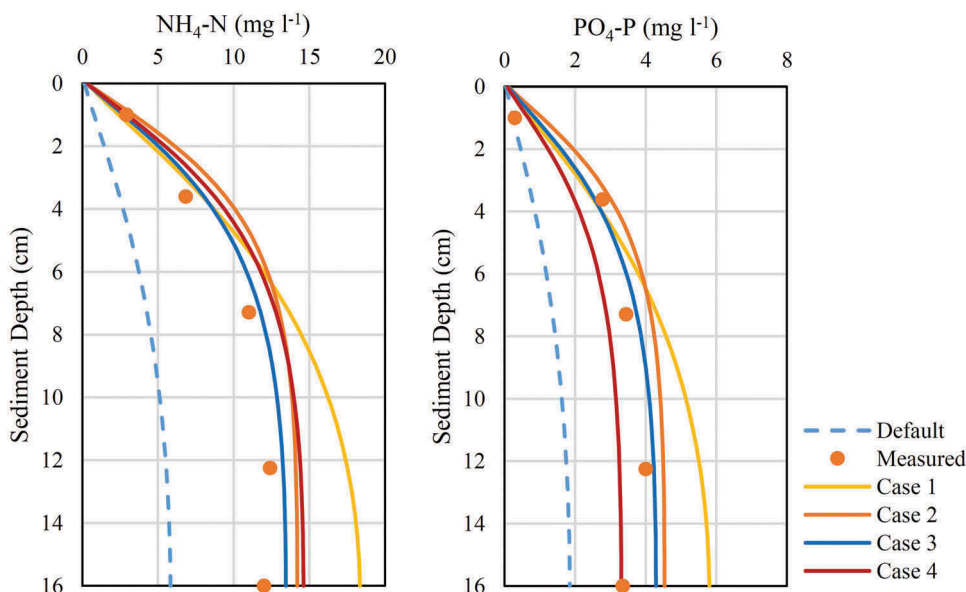


Figure 13. Porewater concentrations of NH₄-N (left) and PO₄-P (right) at Sta. S2.

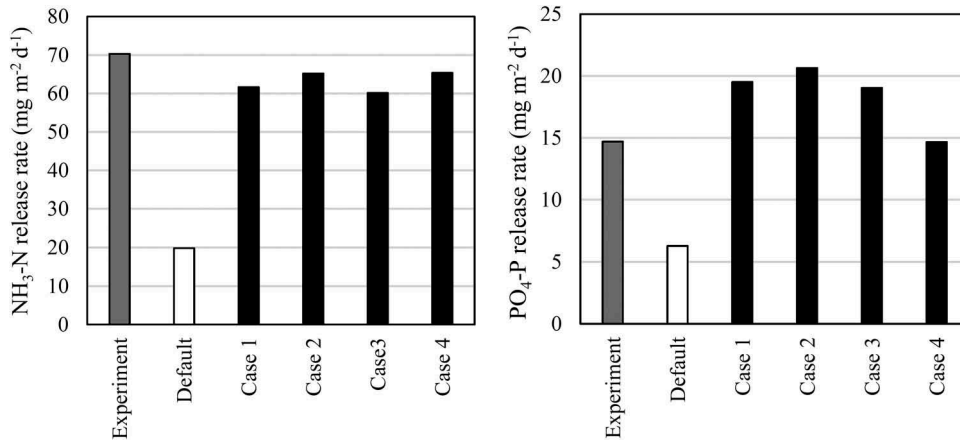


Figure 14. Release rate comparison between experiment value and simulation results using model parameter sets of default values (values in previous studies) and sequentially estimated values at Sta. 2.

phorus between seawater and bottom mud at the same time. Kasih et al. (2009) cannot very well reproduce the vertical profiles of $\text{NH}_4\text{-N}$ and $\text{PO}_4\text{-P}$ in porewater together, but this study obtains better reproducibility by optimization of the ratios using PCE. Because the ratios have a wide range for POM in

sea water, and especially in coastal sediment, the parameter estimation is necessary for early diagenesis models to simulate the substances in sediments.

The distance between Sta. S1 and Sta. S2 is 11.1 km, and the water depths at Sta. S1 and S2 are 12 and 19 m, respectively. Sta. S1 is closer to the river

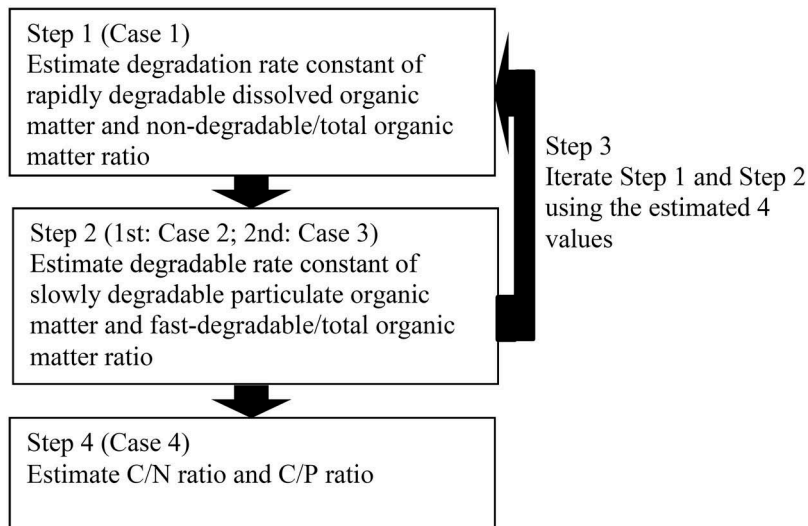


Figure 15. Procedure of parameter estimation in this study.

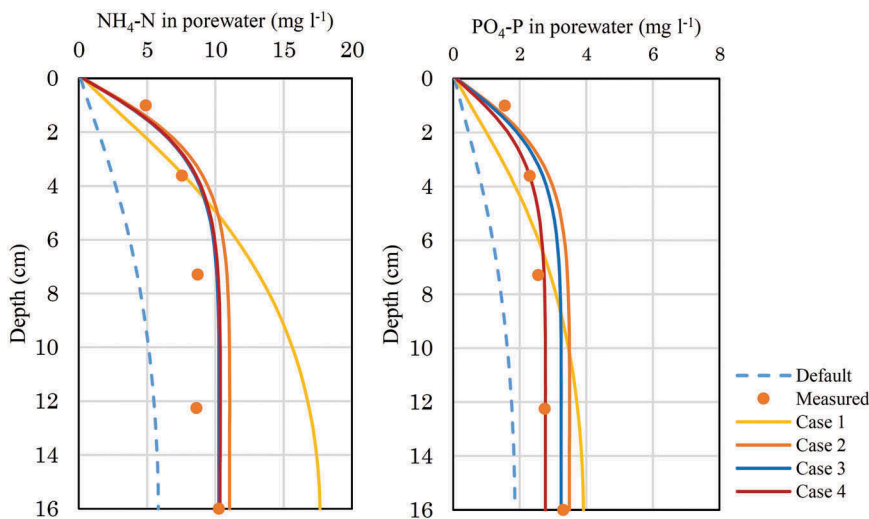


Figure 16. Porewater concentrations of $\text{NH}_4\text{-N}$ (left) and $\text{PO}_4\text{-P}$ (right) at Sta. S1.

Table 6. Comparison of estimated parameters at Sta. S1 and S2.

Parameter	Sta. S1	Sta. S2	Default
KDOM _f	8.5×10^{-2}	9.4×10^{-2}	1.0×10^{-3}
non/t	0.18	0.16	0.2
KPOM _s	4.5×10^{-9}	1.9×10^{-9}	6.0×10^{-10}
fast/t	0.39	0.54	0.57
C/N ratio	9.9	9.2	10
C/P ratio	82.6	90.9	70

mouth of the Yodo River. Although estimated non-degradable OM to total matter ratio is very similar between the sampling sites, fast-degradable OM ratio at Sta. S2 is higher than at Sta. S1. As a result, OM at Sta. S2 consists of more fast-degradable OM; OM at Sta. S1 does of more slowly degradable OM. It is further evidence of this difference that the vertical profile of ignition loss at Sta. S2 is less than at Sta. S1, and the concentration of H₂S in the porewater is high ($\approx 20 \text{ mg l}^{-1}$) in the middle sediment layer at Sta. S2 as well as NH₄-N and PO₄-P.

Estimated rate constants for the mineralization process are much higher than the default values. This means there are more fast-degradable OM deposits in the sediment at the head of Osaka Bay and the nutrient cycle in the water is faster than other areas. It should be noted that all parameters are optimized as constant values over the calculation period of 100 years. This setting is clearly different from the real situation. The parameter values have varied between the period of rapid economic growth and high nutrient loadings, and the last few decades. Because all boundary conditions as well as the model parameters have varied unsteadily, and their temporal change was not surveyed, there is no possible approach to simulate the dynamic change over decades.

5. Summary

In the present study, parameters in an early diagenesis model were estimated using PCE. To utilize the polynomial chaos, sensitivity analyses were performed in advance. While early diagenesis models have wide applicability to the variety of marine sediments, this fact means that a number of model parameters must be calibrated. Additionally, since the dynamics of organic matter in the hydrosphere have been under intense investigation, the fractionation procedure of organic matter to fast and slowly degradable matter has not been definite; the degradation rates of both types of matter should be set up in the model. The observations and experimental results that can define the model parameters, however, are very limited. In most cases, it is necessary to use values from previous studies, which were obtained using other sediment samples in other target areas and surroundings.

Furthermore, in this model, release from sediment is represented by diffusion, which is related to the vertical gradient of material in porewater. Not infrequently, the variation of core samples is so wide that release rates cannot be represented by the conventional diffusion with a single parameter set. Analogical problem like this sometimes occur between the release of nitrogen and phosphorus. In the present study, we propose limiting parameter estimation to six parameters by sensitivity analyses. Although there would be another or more options of parameters that must be estimated, we arrived at the parameters to reproduce the release rates and the vertical profiles of NH₄-N and PO₄-P simultaneously by estimating the ratio of fast-degradable organic matter to total organic matter, the ratio of non-degradable organic matter to total organic matter, the rate constants of fast-degradable DOM and slowly degradable POM, C/N ratio, and C/P ratio. We also propose an optimization procedure that gets acceptable results earlier.

Although we should have considered the verification of boundary conditions, we do not consider optimizing the boundary conditions as well as the extra sets of model parameters in this study. While a PCE method to estimate more than two variables is necessary to implement for simultaneous optimization of both boundary conditions and model parameters in an early diagenesis model, PCE in this study could be used only for estimating the boundary conditions.

Acknowledgments

This work was supported by JSPS KAKENHI Grant Numbers JP25709042 and JP16KK0128. We thank Kyosuke Teranaka for his contribution in the early stage of this study. We are most grateful to the anonymous reviewers and editors for their efforts and valuable comments.

Disclosure statement

No potential conflict of interest was reported by the authors.

Funding

This work was supported by JSPS Kakenhi [JP16KK0128] and [JP25709042].

ORCID

Masayasu Irie  <http://orcid.org/0000-0002-9910-0727>
 Teruhisa Okada  <http://orcid.org/0000-0002-2505-7463>
 Jann Paul Mattern  <http://orcid.org/0000-0002-8291-5161>
 Katja Fennel  <http://orcid.org/0000-0003-3170-2331>

References

- Arndt, S., B. B. Jørgensen, D. E. LaRowe, J. J. Middelburg, R. D. Pancost, and P. Regnier. 2013. "Quantifying the Degradation of Organic Matter in Marine Sediments: A Review and Synthesis." *Earth-Science Reviews* 123: 53–86. doi:10.1016/j.earscirev.2013.02.008.
- Berg, P., S. Rysgaard, and B. Thamdrup. 2003. "Dynamic Modeling of Early Diagenesis and Nutrient Cycling. A Case Study in an Arctic Marine Sediment." *American Journal of Science* 303: 905–955. doi:10.2475/ajs.303.10.905.
- Berner, R. A. 1964. "An Idealized Model of Dissolved Sulfate Distribution in Recent Sediments." *Geochimica et Cosmochimica Acta* 28: 1497–1503. doi:10.1016/0016-7037(64)90164-4.
- Berner, R. A. 1974. "Kinetic Models for the Early Diagenesis of Nitrogen, Sulfur, Phosphorus, and Silicon in Anoxic Marine Sediments." In *Marine Chemistry (The Sea, 5)*, edited by E. D. Goldberg, 427–450. New York, NY: John Wiley and Sons.
- Berner, R. A. 1980. "Early Diagenesis: A Theoretical Approach." In *Princeton University Press*, pp. 256. New Jersey, US: Princeton University Press.
- Blair, N. E., and R. C. Aller. 2012. "The Fate of Terrestrial Organic Carbon in the Marine Environment." *Annual Review of Marine Science* 4: 401–423. doi:10.1146/annurev-marine-120709-142717.
- Boudreau, B. P. 1996. "A Method-of-Lines Code for Carbon and Nutrient Diagenesis in Aquatic Sediments." *Computers & Geosciences* 22 (5): 479–496. doi:10.1016/0098-3004(95)00115-8.
- Boudreau, B. P. 1997. *Diagenetic Models and their Implementation: Modelling Transport and Reactions in Aquatic Sediments*. Berlin: Springer.
- Canfield, D. E. 1994. "Factors Influencing Organic Carbon Preservation in Marine Sediments." *Chemical Geology* 114: 315–329. doi:10.1016/0009-2541(94)90061-2.
- Fossing, H., P. Berg, B. Thamdrup, S. Rysgaard, H. M. Sorensen, and K. Nielsen. 2004. "Model Set-Up for an Oxygen and Nutrient Flux for Aarhus Bay (Denmark)." *National Environmental Research Institute (NERI) Technical Report*, Ministry of the Environment, Denmark, 483.
- Han, D., K. Nakatsuji, and S. Nishida. 2005. "Characteristics of Bottom Sediment and Water-Sediment Interaction in Enclosed Waters." [In Japanese.] *Proceedings of Coastal Engineering, Japan Society of Civil Engineers* 52: 966–970.
- Hopkinson, C. S., and J. J. Vallino. 2005. "Efficient Export of Carbon to the Deep Ocean through Dissolved Organic Matter." *Nature* 433: 142–145. doi:10.1038/nature03191.
- Irie, M., K. Nakatsuji, and K. Teranaka. 2007. "Study of Sediment Quality at Dredged Hollow Places in Port of Han-Nan, Osaka Bay." [In Japanese.] *Proceedings of Coastal Engineering, Japan Society of Civil Engineers* 54: 1091–1095.
- Irie, M., S. Nishida, K. Teranaka, T. Tsuji, and Y. Nakatani. 2011. "Modeling of Anoxic Mineralization Processes in the Sediments of Eutrophic Littoral Regions of Osaka Bay." *The Proceedings of The Twenty-first (2011) International Offshore and Polar Engineering Conference* 879–886. doi: 10.1177/1753193411402762.
- Irie, M., S. Nishida, K. Teranaka, Y. Tsuji, M. Hirasawa, T. Fujiwara, and M. Nakasuji. 2010. "Analysis of Hypoxia Dynamics Using Pelagic and Benthic Biogeochemical Model: Focus on the Formation and Release of Hydrogen Sulfide." [In Japanese.] *Journal of Japan Society of Civil Engineers, Ser. B2 (Coastal Engineering)* 66 (1): 1066–1070. doi:10.2208/kaigan.66.1066.
- Japanese Industrial Standards Committee. 2016. "Japan Industrial Standard", Accessed <https://www.jisc.go.jp/app/jis/general/GnrJISSearch.html>.
- Japan River Association, J. R. 2018. "Rivers in Japan." Accessed 31 May 2018. http://www.japanriver.or.jp/river_law/kasenzu/kasenzu_gaiyou/kinki_r/060yodo.htm.
- Joh, H. 1986. "Studies on the Mechanism of Eutrophication and the Effect of It on Fisheries Production in Osaka Bay." [In Japanese.] *Bulletin of Osaka Prefectural Fisheries Experimental Station* 7: 1–174.
- Kasih, G. A. A., S. Chiba, Y. Yamagata, Y. Shimizu, and K. Haraguchi. 2009. "Numerical Model on the Material Circulation for Coastal Sediment in Ago Bay." *Journal of Marine Systems* 77: 45–60. doi:10.1016/j.jmarsys.2008.11.006.
- Laurent, A., K. Fennel, R. Wilson, J. Lehrter, and R. Devereux. 2016. "Parameterization of Biogeochemical Sediment–Water Fluxes Using in Situ Measurements and a Diagenetic Model." *Biogeosciences* 13: 77–94. doi:10.5194/bg-13-77-2016.
- Martiny, A. C., C. T. A. Pham, F. W. Primeau, J. A. Vrugt, J. K. Moore, S. A. Levin, and M. W. Lomas. 2013. "Strong Latitudinal Patterns in the Elemental Ratios of Marine Plankton and Organic Matter." *Nature Geoscience* 6: 279–283. doi:10.1038/ngeo1757.
- Mattern, J. P., K. Fennel, and M. Dowd. 2012. "Estimating Time-Dependent Parameters for a Biological Ocean Model Using an Emulator Approach." *Journal of Marine Systems* 96–97: 32–47. doi:10.1016/j.jmarsys.2012.01.015.
- Mattern, J. P., K. Fennel, and M. Dowd. 2013. "Sensitivity and Uncertainty Analysis of Model Hypoxia Estimates for the Texas-Louisiana Shelf." *Journal of Geophysical Research: Oceans* 118: 1316–1332.
- Ministry of Environment, Government of Japan. 2016. "Regarding Population Coverage of Sewage Treatment by the End of Fiscal 2016." [In Japanese.] Accessed <http://www.env.go.jp/press/102973.html>.
- Ministry of Land, Infrastructure, Transport and Tourism, Government of Japan. 2017. "Setonaikai Sogo Suishitsu Chosa (Comprehensive Water Quality Survey of the Seto Inland Sea)." [In Japanese.] Accessed 1 May 2017 <http://www.pa.cgr.mlit.go.jp/chiki/suishitu/index.html>.
- Ministry of Land, Infrastructure, Transport and Tourism, Government of Japan. 2018. "Osaka Bay Water Quality Constant Monitoring System" Accessed 31 May 2018, <http://222.158.204.199/obweb/>.
- Nakajima, M., M. Sano, and S. Akiyama. 2016. "Nutrient Release from Sediments of Osaka Bay." [In Japanese.] *Proceedings for Research Workshop* edited by Research Institute of Environment, Agriculture, and Fisheries of Osaka Prefecture. Accessed 31 May 2018. http://www.kan-nousuiken-osaka.or.jp/publication/youshi_suisan.html.
- Nakatani, Y. 2012. "Practical study on pollution loads and material cycle systems in Osaka Bay." [In Japanese.] Doctoral dissertation, Osaka University (available at <http://hdl.handle.net/11094/2090>).
- Nakatani, Y., R. Kawasumi, and S. Nishida. 2011. "Change of Inflow Load and Water Environment in Osaka Bay." *Journal of Japan Society of Civil Engineers, Ser. B2 (Coastal Engineering)* 67 (2): 1_886–1_890. [In Japanese.]. doi:10.2208/kaigan.67.1_886.
- Nakatsuji, K., and T. Fujiwara. 1997. "Residual Baroclinic Circulations in Semienclosed Coastal Seas." *Journal of Hydraulic Engineering* 123 (4): 362–373. doi:10.1061/(ASCE)0733-9429(1997)123:4(362).

- Nishida, S., M. Irie, and K. Nakatsuji. 2006. "Characteristics of Suspended Particulate Matter and Bottom Sediment in the Head of Osaka Bay." [In Japanese.] *Proceedings Journal of Coastal Engineering, Japan Society of Civil Engineers* 53: 991–995.
- Nishida, S., Y. Nakatani, K. Shimada, and M. Irie. 2008. "Water Quality of Rainwater and Its Impact on Primary Production in the Osaka Bay." [In Japanese.] *Proceedings of Coastal Engineering, Japan Society of Civil Engineers* 55: 1061–1065. doi:10.2208/proce1989.55.1061.
- Okaichi, T. 1979. "Cycles of Nitrogen and Phosphorus Surrounding Plankton." *Suiiki no Jijosayo to Joka* [Self-Purification and Sanitization in Water Area], [In Japanese.] edited by the Japanese Society of Fisheries Science, 70–83. Tokyo: Kouseisha-Kouseikaku.
- Soetaert, K., P. M. J. Herman, and J. J. Middelburg. 1996a. "A Model of Early Diagenetic Processes from the Shelf to Abyssal Depths." *Geochimica et Cosmochimica Acta* 60: 1019–1040. doi:10.1016/0016-7037(96)00013-0.
- Soetaert, K., P. M. J. Herman, and J. J. Middelburg. 1996b. "Dynamic Response of Deep-Sea Sediments to Seasonal Variations: A Model." *Limnology and Oceanography* 41: 1651–1668. doi:10.4319/lo.1996.41.8.1651.
- Steenbergh, A. K., P. L. E. Bodelier, M. Heldal, C. P. Slomp, and H. J. Laanbroek. 2013. "Does Microbial Stoichiometry Modulate Eutrophication of Aquatic Ecosystems?." *Environmental Microbiology* 15: 1572–1579. doi:10.1111/emi.2013.15.issue-5.
- Tada, K., T. Nishikawa, K. Taruya, K. Yamamoto, K. Ichimi, K. Yamaguchi, and T. Honjo. 2014. "Nutrient Decrease in the Eastern Part of the Seto Inland Sea and Its Influence on the Ecosystem's Lower Trophic Levels." [In Japanese.] *Bulletin on Coastal Oceanography* 52 (1): 39–47.
- Van Cappellen, P., and Y. Wang. 1995. "Metal Cycling in Surface Sediments: Modeling the Interplay of Transport and Reaction." In *Metal Contaminated Sediments*, edited by H. E. Allen, 21–64, Michigan, US: Ann Arbor Press.
- Van Cappellen, P., and Y. F. Wang. 1996. "Cycling of Iron and Manganese in Surface Sediments: A General Theory for the Coupled Transport and Reaction of Carbon, Oxygen, Nitrogen, Sulfur, Iron, and Manganese." *American Journal of Science* 296: 197–243. doi:10.2475/ajs.296.3.197.
- Van der Weijden, C. H. 1992. "Chapter 2 Early Diagenesis and Marine Pore Water." *Developments in Sedimentology* 47: 13–134. in *Diagenesis*. III, Elsevier. doi:10.1016/S0070-4571(08)70564-8.
- Wang, Y., and P. van Cappellen. 1996. "A Multicomponent Reactive Transport Model of Early Diagenesis: Application to Redox Cycling in Coastal Marine Sediments." *Geochimica et Cosmochimica Acta* 60: 2993–3014. doi:10.1016/0016-7037(96)00140-8.
- Wiener, N. 1938. "The Homogeneous Chaos." *American Journal of Mathematics* 60 (4): 897–936. doi:10.2307/2371268.
- Wijsman, J. W. M., P. M. J. Herman, J. J. Middelburg, and K. Soetaert. 2002. "A Model for Early Diagenetic Processes in Sediments of the Continental Shelf of the Black Sea." *Estuarine, Coastal and Shelf Science* 54: 403–421. doi:10.1006/ecss.2000.0655.
- Wilson, R. F., K. Fennel, and P. Mattern. 2013. "Simulating Sediment-Water Exchange of Nutrients and Oxygen: A Comparative Assessment of Models against Mesocosm Observations." *Continental Shelf Research* 63: 69–84. doi:10.1016/j.csr.2013.05.003.
- Xiu, D., and G. E. Karniadakis. 2002. "The Wiener–Askey Polynomial Chaos for Stochastic Differential Equations." *SIAM Journal on Scientific Computing* 24 (2): 619–644. doi:10.1137/S1064827501387826.
- Xiu, D., and G. E. Karniadakis. 2003. "Modeling Uncertainty in Flow Simulations via Generalized Polynomial Chaos." *Journal of Computational Physics* 187 (1): 137–167. doi:10.1016/S0021-9991(03)00092-5.
- Yokoyama, H., and M. Sano. 2015. "Zoning of Osaka Bay Based on Principal Component Analysis of Sediment Parameters and Comparison between the 2013 and Previous Surveys." [In Japanese.] *Nippon Suisan Gakkaishi* 81 (1): 68–80. doi:10.2331/suisan.81.68.